26

TOWARD A RATIONAL SOLVENT SELECTION FOR CONFORMATIONAL POLYMORPH SCREENING

YURIY A. ABRAMOV, MARK ZELL, AND JOSEPH F. KRZYZANIAK
Pfizer Global Research & Development, Pharmaceutical Sciences, Groton, CT, USA

26.1 INTRODUCTION

Crystalline solids with the same chemical composition but different molecular arrangements in the crystal lattice are known as polymorphs [1]. Changes in polymorphic form during pharmaceutical development can have a negative impact on a drug's performance, that is, solubility and bioavailability (Chapter 25), chemical and physical stability, and mechanical properties. Therefore, it is necessary to identify the stable crystal form under normal manufacturing and storage conditions to ensure that this form does not change during the life cycle of the drug product.

Polymorph screens are conducted early in drug development to identify unique crystal forms of the active pharmaceutical ingredient (API). Each crystal form discovered is characterized to identify whether the crystalline phase is an anhydrous form or a solvate. The polymorphic lattice can also consist of either the same or the different molecular conformations. Conformational polymorphism describes the latter case when different conformations of the same molecule occur in different crystal forms [2]. Solid-state characterization studies are then conducted to develop an understanding of the stability relationship between all crystalline phases since the thermodynamically stable form is directly related to conditions (crystallization, environmental, and manufacturing) in which the API is exposed to during the drug development process [1].

During the preparation of the desired polymorphic form, the science of crystallization has shown to be a very complex phenomenon that is dictated by interplay between different thermodynamic and kinetic factors. The presence of different molecular conformations in saturated solution introduces an additional degree of complexity allowing crystallization of polymorphs different not only in the packing arrangement but also in the molecular geometry as seen in conformational polymorphs [1–3]. Crystallization is believed to be a multiple stage process in which molecules associate into prenucleation molecular clusters followed by their assembling into crystal nuclei leading to crystal growth (Figure 26.1) [3, 4]. It was assumed [5] and later demonstrated [6, 7] that a saturated phase contains clusters of molecules displaying packing of all possible polymorphs. Final growth of a specific polymorph can be achieved by altering crystallization conditions, such as degree of supersaturation, type of solvent, and additives [8–11].

From a thermodynamic viewpoint, a primary factor for conformational polymorph formation is stabilization of the conformer free energy in the crystalline environment relative to that in saturated solution. That consideration defines the type of solvent as one of the major factors in polymorphic selectivity. Solvent selection for polymorph crystallization is usually based on achieving a reasonably high API solubility [12] to facilitate crystal growth during drowning-out, evaporative, cooling, or slurry crystallization techniques. With this, it is reasonable to assume that a higher population of a specific molecular conformation is needed to feed a crystallization of a corresponding conformational polymorph. A higher conformer population should contribute to increased nucleation of the corresponding conformational polymorph, structural organization of which is most readily

Chemical Engineering in the Pharmaceutical Industry: R&D to Manufacturing Edited by David J. am Ende

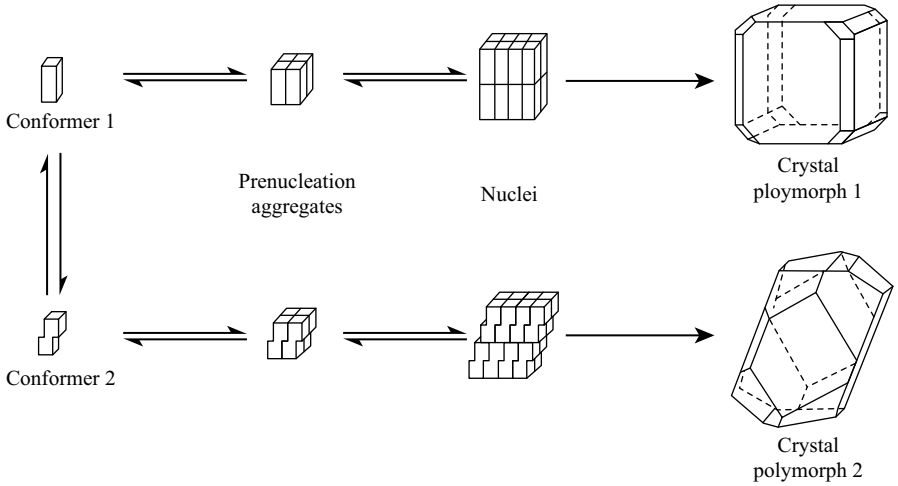

FIGURE 26.1 An illustration of the crystallization of conformationally flexible molecules. Reproduced from Ref. 3 with permission. Copyright (2010) American Chemical Society.

derived from the preferred conformations in solution [13, 14]. The focus of this chapter is testing a computational approach for conformational population prediction in different solvent media in order to explore diversification of conformational populations in solution. A working hypothesis is that controlling the selective conformer's population should facilitate a rational solvent selection for conformational polymorph screening. In addition, prediction of conformer population in a supercooled liquid (self-media) will also be performed and should mimic stabilization of molecular conformations in an amorphous solid state. An assumption is made that while the conformer distribution in solution is important for nucleating a conformational polymorph, a high conformation population in the supercooled liquid should reflect stability of the conformation in a solid state neglecting long-order contributions. The interplay between conformer distribution in solution and self-media should reflect a driving force for crystallization of the different molecular conformations.

In addition, the proposed conformational population analysis technique will be discussed for preferable conformation selection for crystal structure prediction (CSP). CSP is an important computational tool that is valuable not only in guiding polymorph screening [15–17] but also in performing a polymorphic risk assessment for solid form nomination during pharmaceutical development [18]. However, the currently available CSP methods heavily rely on a correct selection of the starting molecular conformations that are typically held rigid at least during initial crystal packing generation. That is why a rational selection of the preferred starting molecular conformations for CSP of complex flexible molecules is of great importance [19–21].

Although important, the following topics and considerations are out of scope of this chapter.

1. Due to the effect of different crystalline environments, molecular conformations may be distributed around local minima of the potential energy surface as defined in the reference media (e.g., gas phase) [22]. Molecular conformations considered in this chapter are defined strictly by a local minimum in the aqueous or gas media neglecting crystal packing effects. Therefore, we will be considering different types of conformations representing possible conformers with slightly different geometries. This is especially true for the freely rotatable bonds, rotation of which is defined by a flat potential energy surface in the gas phase or in the implicit solution, while torsion angle of such bonds may be fixed in a crystalline environment by a specific hydrogen-bonding interaction (e.g., hydroxyl and carboxyl groups).
2. Relative stability of polymorphs is described by an equilibrium-phase diagram and cannot be adequately determined by the methods developed in this chapter. Moreover, the intention of this chapter is to facilitate crystallization of a diverse set of conformational polymorphs including those that are metastable.
3. Rotational barriers that are important for kinetics of conformational interconversion will not be considered. Therefore, only thermodynamic factors will be used in theoretical evaluation of the conformational distributions.
4. In addition, no considerations of kinetic factors that may affect selectivity of the polymorph crystallization will be addressed. Among such factors are the degree of supersaturation, cooling and stirring rates, impurities and additives that affect the polymorphic form, morphology, and crystal growth [8–11].

26.2 METHODS

26.2.1 Theoretical

The conformational population study was performed in two steps. During the first step, a stochastic conformational search was performed using the MOE 2008.10 software package [23] with the following parameters: MMFF94× force field with distance-dependent dielectric, chiral constrains, allowing amide-bond rotation and energy cutoff of 7 Kcal/mol. After the conformational search was complete, the conformations generated were further optimized using aqueous media at PBE/DNP/COSMO level of theory (defined by theoretical method and a basis set) as implemented in DMol^3 [24–26]. This utilizes density functional theory (DFT) PBE approximation [27] with all-electron double-numeric-polarized basis set. The effect of bulk water is estimated by conductor-like screening model (COSMO) as implemented in DMol^3 [28]. It was demonstrated recently [29] that PBE is one of the best DFT functionals in prediction of energies of hydrogen-bonding (HB) systems. The *cosmo* files generated by the PBE/DNP/COSMO calculations for each conformer are further used for solvation free energy calculations, ΔG_{solv}, and for prediction of conformational distribution in different solvents adopting COSMO-RS theory [30] as implemented in COSMOtherm software [31].

An obvious advantage of the application of the PBE/DNP/COSMO calculations is that the COSMOtherm parameters are specifically optimized for this level of theory. However, the DFT is known to underestimate strong electron correlation effects (such as dispersion energy) [32]. Therefore, in order to assure the quality of the PBE/DNP calculations, we have also performed calculations at a combined level of theory according to the following procedure (Chapter 24). The conformer free energy in solution is presented as

$$G(i) = E_{\text{gas}}(i) + \text{ZPE}(i) + \Delta G_{\text{solv}}(i) \tag{26.1}$$

where $E_{\text{gas}}(i)$ is the gas-phase energy of the conformer and ZPE(i) is its zero-point vibrational energy. The value of $\Delta G_{solv}(i)$ is calculated at the PBE/DNP/COSMO level as described above, while the gas free energy of the conformer was calculated at the RI-MP2/TZVPP level [33] adopting TURBOMOLE software [34]. The ZPE(i) contribution was estimated at the DMol^3 PBE/DND level of theory.

In the following discussions, the two theoretical approaches described above for simplicity will be referred to as PBE and RI-MP2 levels, respectively.

The equilibrium conformer population, $p(i)$, was calculated according to the following equation [30]:

$$p(i) = \frac{\varpi(i)\exp(-G(i)/RT)}{\sum_j \varpi(j)\exp(-G(j)/RT)} \tag{26.2}$$

where $\varpi(i)$is a multiplicity of the conformer i, which is based on the geometrical degeneration factors, R is the universal gas constant and T is the temperature in Kelvin. A challenge in an accurate prediction of $p(i)$ is introduced by an exponential dependence on the calculated $G(i)$ values, so that a relatively small error in conformer's free energy transforms into significant errors in conformer populations. For example, in case of a simple system with two conformations displaying similar energies and multiplicities, the true population of each conformer is 50%. However, an error in predicted relative $G(i)$ values, $G(2) - G(1)$, of 0.4 kCal/mol would result in $p(i)$ error at the room temperature of $\pm 16.3\%$. The predicted conformer populations would be 66.3% and 33.7%.

26.2.2 Experimental

26.2.2.1 NMR Measurements ^{1}H, gHMBC, and G-BIRD$_{R,X}$-CPMG-HSQMBC experiments were performed on a Bruker Avance DRX 600 spectrometer equipped with a 5 mm BBO probe with z-axis gradient. All experiments were performed at a temperature of 298 K.

Samples were prepared at concentrations of 10, 100, and 300 mg/mL in acetone-d_6, acetonitrile-d_3, and methanol-d_4 with tetramethylsilane as an internal standard. All experiments were performed using Bruker standard pulse sequences, except for G-BIRD$_{R,X}$-CPMG-HSQMBC, which was written and implemented by a staff member in our laboratory.

For ^{1}H NMR analysis, typically one transient was acquired with a 1s relaxation delay using 32 K data points. The 90° pulse was 10.5 μs and a spectral width of 10775 Hz was used.

The gHMBC spectrum was acquired with 4096 data points for $F2$ and 128 $F1$ increments. gHMBC data was acquired with 4K data points in $F2$, 128 increments for $F1$ (16 scans per increment) and $F2 \times F1$ spectral window of 5200×23800 Hz. Data were processed with 4K data points zero-filled to 8K in $F2$ and 128 data points zero-filled to 1K in $F1$.

The G-BIRD$_{R,X}$-CPMG-HSQMBC spectra were acquired in approximately 14 h with 4K data points in $F2$, 128 increments for $F1$ with 256 scans per increment and $F2 \times F1$ spectral window of 5200×23800 Hz. Data were processed with 4K data points zero-filled to 8K in $F2$ and 128 data points zero-filled to 1K in $F1$. A sine squared window function was applied to the $F1$ dimension before Fourier transformation and no apodization was applied in the $F2$ dimension. The gradient ratios for G-BIRD$_{R,X}$-CPMG-HSQMBC were G1:G2:G3:G4:G5 = 2.5:2.5:8:1: +/−2. The delay for long-range polarization transfer was set to 63 ms. The delay used for (delta) was set to 200 μs. All measured coupling constants are believed to be within +/−0.5 Hz. The values of $^3J_{\text{CH}}$

were determined from direct measurement and subsequent manual peak fitting analysis [35].

26.3 RESULTS AND DISCUSSION

26.3.1 Test of Accuracy of Conformational Population Predictions

The accuracy of conformational population prediction for flexible organic molecules was tested at different levels of theory. For this, three test cases were selected consisting of *N*-substituted amides series [36], *N*-(pyridin-2-yl)benzamides chemical series [37], and *S*-ibuprofen. While accurate experimental conformational populations based on the solution NMR experiments were available for the two first cases, a separate experimental work was performed for *S*-ibuprofen.

26.3.1.1 N-Substituted Amides Series Yamasaki et al. [36] reported a detailed study of the *cis–trans* ratio of conformer population of a series of *N*-substituted amides (Figure 26.2) in DCM-d_2, methanol-d_4, and acetone-d_6 at 183 K. It was demonstrated that the compounds **1** and **2** display *trans* and *cis* conformations in all three solvents, respectively. A very weak solvent dependence was found for the compounds **6** and **7**, the former being preferably in the *cis*-conformations while the latter displaying close to a uniform *cis–trans*-distribution. The most remarkable result of the study was an observation of a pronounced solvent dependent conformational switching of the phenylhydroxamic acids (**3**–**5**) (Figure 26.3) (Table 26.1) from the predominantly *cis*-conformations in DCM to preferably *trans*-conformations in acetone.

Theoretical predictions at the DFT (PBE) and RI-MP2 levels are in agreement with the experimental observations (Table 26.1). In particular, the strong solvent dependence of conformations of the compounds **3**–**5** was reproduced correctly, although the absolute values of *cis*-populations in methanol and acetone are underestimated for the compounds **3** and **4**, especially by the DFT method (Figure 26.3). At the same time, both levels of the predictions overestimated *cis*-populations of the compound **7**. The overestimation is more pronounced in the case of the predictions using the RI-MP2 level of theory.

26.3.1.2 N-(Pyridin-2-yl)Benzamides Series Populations of *cis* conformations of a series of *N*-(pyridin-2-yl) benzamides (**8**–**11**) (Figure 26.4) as well as of *N*-(2,6-dimethylphenyl)acetamide (**12**) (Figure 26.4) were studied by means of solution NMR spectroscopy in three solvents: chloroform-d_1, methanol-d_4, and acetone-d_6 at 243 K (Table 26.2) [37]. It was demonstrated that the compounds **8** and **10** display *trans*- and *cis*-conformations in all three solvents, respectively. These observations are analogous

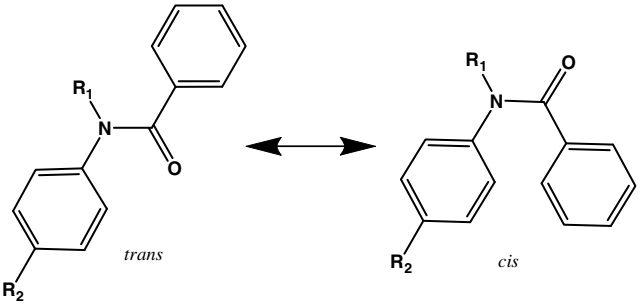

1. $R_1 = H$, $R_2 = H$
2. $R_1 = CH_3$, $R_2 = H$
3. $R_1 = OH$, $R_2 = H$
4. $R_1 = OH$, $R_2 = CH_3$
6. $R_1 = NH_2$, $R_2 = H$
7. $R_1 = OCH_3$, $R_2 = H$

5.

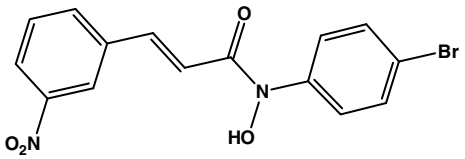

FIGURE 26.2 Chemical structures of *N*-substituted amides series [36].

to the results reported by Yamasaki et al. [36] for the compounds **1** and **2** (Figure 26.2) (Table 26.1). Solvent-dependent conformational behavior was observed for the compounds **9** and **12**. Theoretical predictions at the DFT PBE level are in a quite good agreement with the experimental observations (Table 26.2). In particular, the solvent dependence of the compounds **9** and **12** conformations was reproduced correctly, although the absolute values of *cis*-populations in methanol and acetone are somewhat overestimated (Figure 26.5). The overestimation is more pronounced in case of the predictions at the RI-MP2 level of theory.

It is found for both *N*-substituted amides and *N*-(pyridin-2-yl)benzamides series that a combined approach with RI-MP2/TZVPP gas-phase calculations does not demonstrate an advantage over PBE/DNP/COSMO level of theory in predicting conformational distributions in different solvents. Therefore, a less demanding PBE/DNP/COSMO analysis was adopted for further calculations.

EXAMPLE 26.1 *S*-IBUPROFEN CONFORMATIONAL POPULATION IN METHANOL, ACETONE, AND ACETONITRILE

Ibuprofen is a nonsteroidal anti-inflammatory drug in which activity is usually associated to the *S*(+)-isomer. As shown in Figure 26.6, the ibuprofen molecule displays four flexible

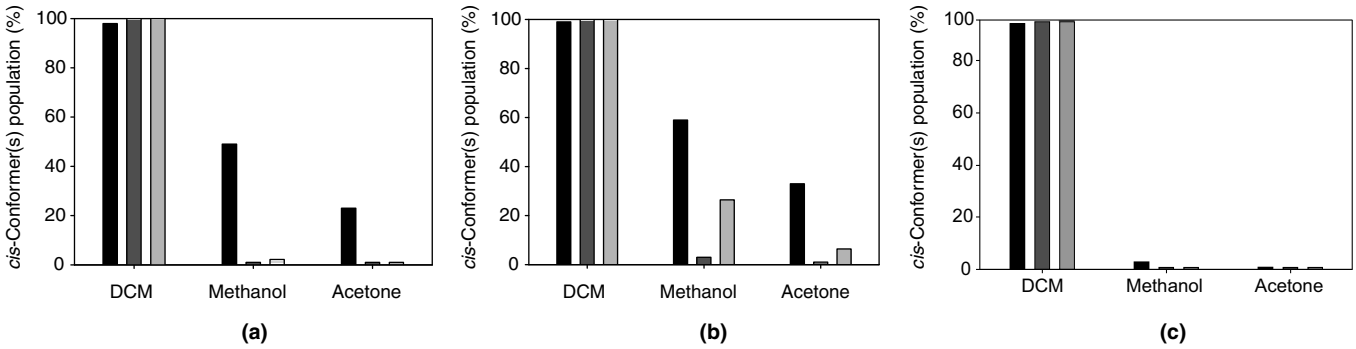

FIGURE 26.3 *cis*-Conformer(s) populations of the compounds **3–5** ((a)–(c)) of *N*-substituted amides series (Table 26.1) (Figure 26.2) [36]. Experimental, PBE, and RI-MP2 results are represented by black, dark gray, and gray bars, respectively.

torsion angles. The initial stochastic conformational search was performed using the MOE software package [23] adopting default parameters (MMFF94× force field with distance-dependent dielectric, chiral constrain, and energy cutoff of 7 Kcal/mol). The 25 lowest energy conformations generated were further optimized in water at the PBE/DNP/COSMO level of theory. The optimized *S*-ibuprofen conformations are aligned and presented in Figure 26.7. The *cosmo* files generated were used for the conformational distribution study in methanol, acetone, and acetonitrile solvents at 25°C, adopting COSMOtherm software [31]. No significant solvent effect on conformer distribution was found. Population of four conformers (Figure 26.8) was found to be in the range of 12–23% in all solvents under consideration, which significantly exceeded the population of any other conformation. The torsion angles of the preferred conformations are listed in Table 26.3. However, it should be expected that in a crystalline environment, the angle τ_1 may change (e.g., switch by $\sim$180°) in order to accommodate intermolecular hydrogen-bonding interaction.

The solvent and concentration dependences of *S*-ibuprofen conformations were investigated by G-BIRD$_{R,X}$-CPMG-HSQMBC experiment. For this, the $^3J_{CH}$ heteronuclear coupling constants that define the flexible torsion angles (τ_1–τ_4) in the *S*-ibuprofen molecule were extracted (Table 26.4). Due the fast conformational interconversion at the room temperature, the NMR observations are averaged over specific conformational distributions.

The $^3J_{CH}$ coupling constant data presented in Table 26.4 suggest that there is no change in the molecular conformation of *S*-ibuprofen in solution, within the limits of the NMR measurements ($> +/-0.5$ Hz) as a function of either solvent composition or concentration. This data further support the computational results for *S*-ibuprofen presented above that also suggest no change in conformational populations as a function of solvent composition. An exercise of converting the measured $^3J_{CH}$ coupling constant values into their respective torsion angles was not carried out.

26.3.2 Conformational Distribution and Polymorph Crystallization

Polymorph crystallization may be performed by utilizing different crystallization techniques. Typically a slurry experiment is considered to be the best to induce solvent-mediated transformation to the most stable form [38, 39]. The system is

TABLE 26.1 Experimental [36] and Predicted *cis*-Conformers Populations (%) of *N*-Substituted Amides (Figure 26.2) at −90°C in Three Solvents

	DCM			Methanol			Acetone			Self	
Compound	Experimental	PBE	RI-MP2	Experimental	PBE	RI-MP2	Experimental	PBE	RI-MP2	PBE	T (°C)
1	<1	<1	<1	<1	<1	<1	<1	<1	<1	<1	−90
2	98	98.8	>99	>99	95.4	>99	>99	98.8	>99	97.0	−90
3	98	>99	>99	49	<1	2.2	23	<1	<1	98.1	−90
4	>99	>99	>99	59	3.0	26.4	33	<1	6.4	98.6	−90
5	>99	>99	99.6	3	<1	<1	<1	<1	<1	79.6	−90
6	98	>99	>99	95	86.5	>99	85	60.2	>99	97.2	−90
7	50	88.1	>99	63	88.7	>99	55	52.2	>99	45.5	−90

Details of the theoretical approaches based on PBE and RI-MP2 levels of theory are described in Section 26.2.1.

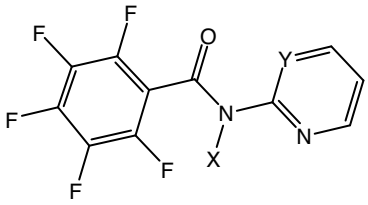

8. X= H, Y = CH
9. X= H, Y = N
10. X = CH_3, Y = N

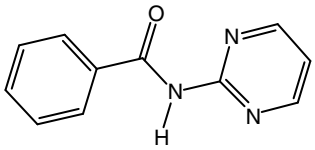

11

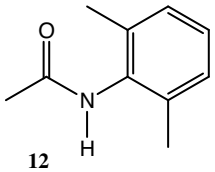

12

FIGURE 26.4 A series of *N*-(pyridin-2-yl)benzamides (**8–11**) and *N*-(2,6-dimethylphenyl)acetamide (**12**) [37].

preferably under thermodynamic control and the solution is saturated with respect to a metastable form and supersaturated with respect to a more stable form. It has been shown that a solvent that gives high solubility provides faster transformation to the most stable form and usually 8 mM solubility threshold has been adopted when designing the slurry experiment [39]. At the same time, cooling and evaporation crystallization in general produces a supersaturated solution with respect to all possible forms, and the system is preferably under kinetic control. In that case, polymorph crystallization typically follows Ostwald law of stages [40] and crystallization of the least stable form is expected first, followed by transformation to a more stable polymorph. The focus of this chapter is to explore a correlation between conformational polymorph distributions and conformational polymorph crystallization. Unfortunately, there is very limited information available in the literature addressing the effect of solvent on both conformational distribution and crystallization. In the following, we will consider four examples—two slurry and two cooling crystallization experiments, for which conformational distribution in different solvents will be predicted by adopting theoretical approaches described above (PBE/DNP/COSMO level of theory).

26.3.2.1 **N-*Phenylhydroxamic Acids*** Experimental and conformational distributions of *N*-phenylhydroxamic acids in three different solvents were reported by Yamasaki et al. [36] and discussed above (Table 26.1, compounds **3–5**). Both NMR spectroscopy and theoretical calculations (Table 26.1, compounds **3–5**) demonstrated that all *N*-phenylhydroxamic acids display switching from the *cis*-conformations in dichloromethane to the *trans*-conformations in methanol and especially in acetone (183 K). Yamasaki et al. recrystallized compound **3** from DCM and acetone producing polymorphs with *cis* (crystal A)- and *trans* (crystal B)-molecular conformations, respectively (Figure 26.9). It appears from differential scanning calorimetry (DSC) profile [36] that an enantiotropic relationship exists between A and B forms so that at room temperature the crystal B is presumably more stable. The stability assignment is opposite to the one that may be based on the predicted population distribution in the self-media (or an amorphous solid, Table 26.1). This reflects the importance of the long-range order contributions in the *N*-phenylhydroxamic acid crystals. An important conclusion from the results of the Yamasaki et al. study [36] is that the polymorph crystallization in different solvents may follow the conformational population trend rather than the Ostwald rule of stages.

26.3.2.2 ***Taltirelin*** Taltirelin ((4*S*)-*N*-[(2*S*)-1-[(2*S*)-2-carbamoylpyrrolidin-1-yl]-3-(3*H*-imidazol-4-yl)-1-oxopropan-2-yl]-1-methyl-2,6-dioxo-1,3-diazinane-4-carboxamide),

TABLE 26.2 Experimental [37] and Predicted *cis*-Conformers Populations (%) of *N*-(Pyridin-2-yl)Benzamides (8–11) (Figure 26.4) and *N*-(2,6-Dimethylphenyl)Acetamide (Figures 26.4 and 26.5) at −30°C in three solvents

	$CHCl_3$			Methanol			Acetone			Self	
Compound	Experimental	PBE	RI-MP2	Experimental	PBE	RI-MP2	Experimental	PBE	RI-MP2	PBE	*T* (°C)
8	<1	<1	<1	<1	<1	<1	—	<1	<1	<1	−30
9	60.6	51.7	66.5	7.4	26.1	56.3	50.3	78.2	96.4	80.0	−30
10	>99	>99	>99	—	>99	>99	—	>99	>99	>99	−30
11	<1	<1	8.4	—	<1	1.3	—	<1	32.4	<1	−30
12	20.6	25.4	35.9	—	7.0	7.8	2.9	3.3	4.2	8.3	−30

Details of the theoretical approaches based on PBE and RI-MP2 levels of theory are described in the Section 26.2.1.

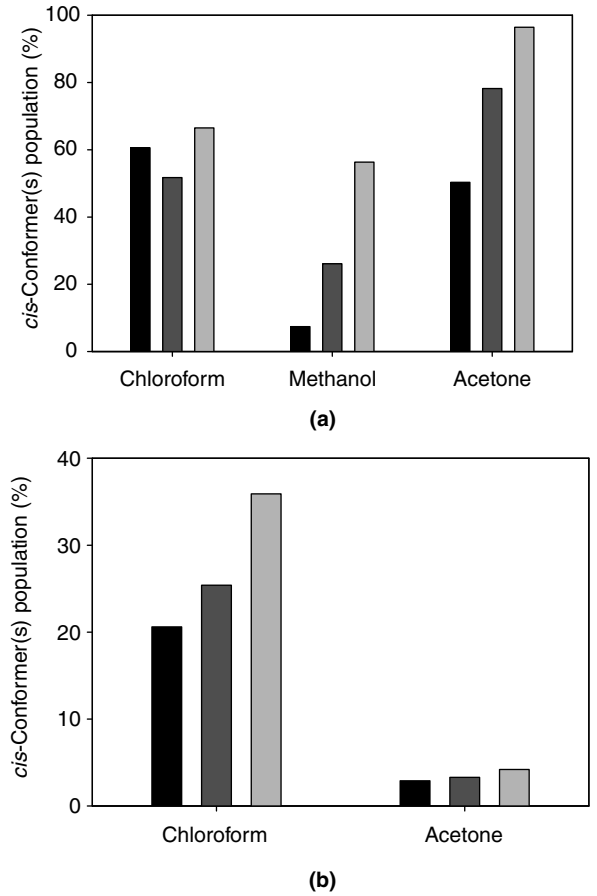

FIGURE 26.5 *cis*-Conformer(s) populations of (a) 2,3,4,5,6-pentafluoro-*N*-(pyrimidine-2-yl)benzamide (**9**) (Table 26.2) (Figure 26.4) and (b) *N*-(2,6-dimethylphenyl)acetamide (**12**) (Table 26.2) (Figure 26.4) [37]. Experimental, PBE, and RI-MP2 results are represented by black, dark gray, and gray bars, respectively.

a central nervous system activating agent, was reported to have two crystalline tetrahydrate forms: a metastable α-form and stable β-form (Figure 26.10) [41, 42]. It was found that the solvent-mediated transformation to the β-form occurring in the water slurry can be significantly promoted by adding a

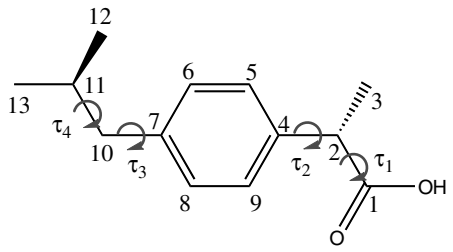

FIGURE 26.6 Structure of ibuprofen molecule with four flexible torsion angles. τ_1: O–C_1–C_2–C_4; τ_2: C_1–C_2–C_4–C_9; τ_3: C_8–C_7–C_{10}–C_{11}; τ_4: C_7–C_{10}–C_{11}–C_{13}.

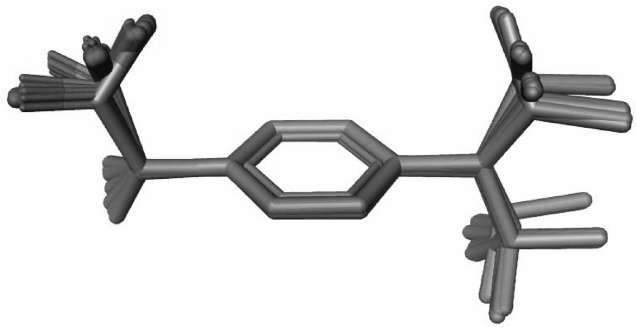

FIGURE 26.7 Aligned 25 *S*-ibuprofen conformations optimized in water at PBE/DNP/COSMO level of theory. All hydrogens are omitted.

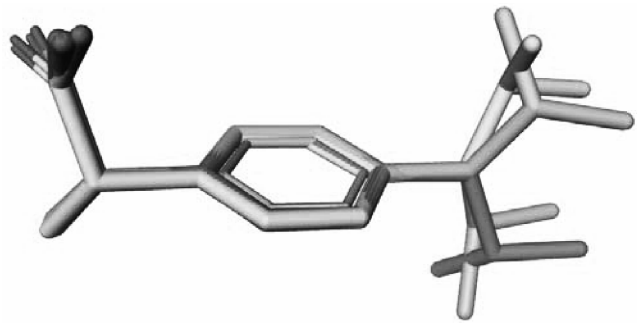

FIGURE 26.8 Aligned four *S*-Iibuprofen conformers that displayed the highest populations in methanol, acetone, and acetonitrile solvents at 25°C.

small amount (10 wt%) of MeOH. It was demonstrated that although the polymorph solubility had little affect with the added MeOH (it is actually slightly decreasing), an increase in methanol concentration causes an induction period of transformation to become shorter. In addition, Shoji Maruyama and Hiroshi Ooshima [42] demonstrated by means of nOe NMR analysis that MeOH causes the conformation change of taltirelin from the α-form to the β-form conformers through the solute-MeOH interaction. That observation supports the importance that the conformer population has on driving the corresponding conformational polymorph crystallization.

Taltirelin is a very flexible molecule with eight rotatable bonds, which makes a reliable conformation search a very challenging task. In order to test whether the MeOH effect on conformational populations can be predicted, the following calculations were performed. The α-form conformation was taken from the crystal structure available in the Cambridge Structure Database [43] (CSD, reference code REPLIH[1]).

[1] REPLIH conformer represents a mirror image ((4R)-*N*-[(2*R*)-1-[(2*R*)-2-carbamoylpyrrolidin-1-yl]-3-(3*H*-imidazol-4-yl)-1-oxopropan-2-yl]-1-methyl-2,6-dioxo-1,3-diazinane-4-carboxamide tetrahydrate) of taltireline α-form as it is described in Refs 41 and 42.

TABLE 26.3 Torsion Angles (Figure 26.6) of the Selected Four Conformations of *S*-ibuprofen with the Highest Populations in the Three Solvents

Conformer	τ_1 (Degrees)	τ_2 (Degrees)	τ_3 (Degrees)	τ_4 (Degrees)
1	94.7	−65.6	−73.1	−63.2
2	96.0	−62.7	−105.3	−173.2
3	95.8	−64.2	103.6	−65.5
4	107.3	−65.7	71.8	−172.8

TABLE 26.4 $^3J_{CH}$ Values (in Hertz) Obtained with the G-BIRD$_{R,X}$-CPMG-HSQMBC Experiment for Ibuprofen in Acetone-d_6, Acetonitrile-d_3, and Methanol-d_4.

Correlation	$^3J_{CH}$ (Hz)								
	CD_3OD 300 mg/mL	CD_3OD 100 mg/mL	CD_3OD 10 mg/mL	CD_3CN 300 mg/mL	CD_3CN 100 mg/mL	CD_3CN 10 mg/mL	$(CD_3)_2CO$ 300 mg/mL	$(CD_3)_2CO$ 100 mg/mL	$(CD_3)_2CO$ 10 mg/mL
H_3-C_4	4.6	4.6	4.5	4.4	4.5	4.5	4.6	4.7	4.7
H_8-C_1	5.1	5.0	5.1	5.1	5.0	5.1	5.1	5.1	5.1
$H_{12(13)}-C_{10}$	4.7	4.6	4.7	4.8	4.7	4.6	4.7	4.7	4.7
$H_{11}-C_7$	2.5	2.4	2.4	2.5	2.4	2.4	2.5	2.5	2.3

The numbering scheme is similar to the one presented in Figure 26.6.

The β-form conformation was reconstructed from that of α-form by rotation of two single bonds as described in the literature (Figure 26.10) [41, 42]. The α- and the β-form conformations were further adopted for the conformational population analysis at the PBE/DNP/COSMO level of theory. Although no significant effect was reproduced at 10%wt MeOH concentration, the calculations demonstrated a general qualitative increase of the β-conformer population when switching from aqueous to methanol solution (Figure 26.11).

26.3.2.3 Famotidine Famotidine, a histamine H2-receptor antagonist, is a very flexible molecule that has two known conformational polymorphs: A and B. These two polymorphs are monotropically related with form A being more stable [44]. Since form B is the metastable form, it is kinetically favored and according to the Ostwald law should crystallize first when cooling a saturated solution. Selective cooling crystallization of Famotidine polymorphs was reported by Lu et al. [44]. It was found that the form prepared

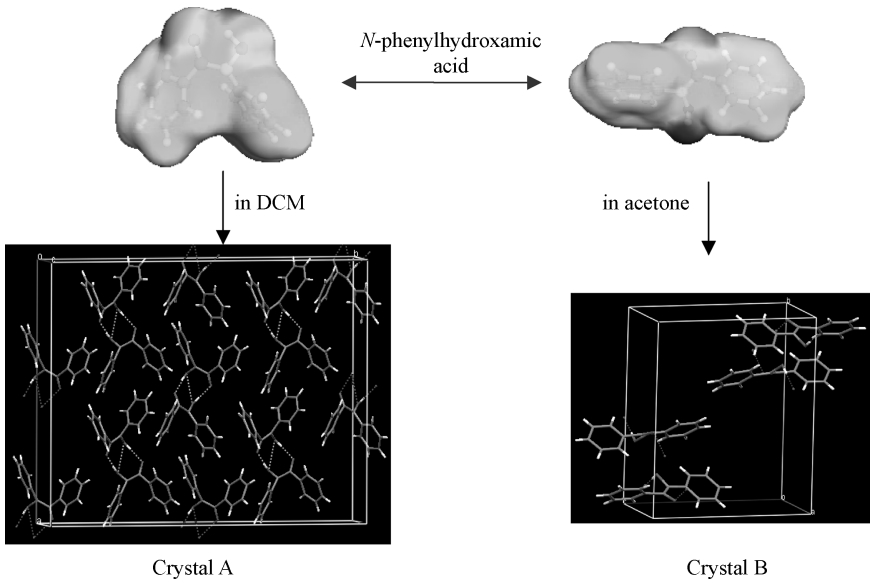

FIGURE 26.9 Conformational equilibrium of *N*-Phenylhydroxamic acid (**3**) (Table 26.1) and crystal structures from recrystallization in DCM (crystal A) and acetone (crystal B) [36].

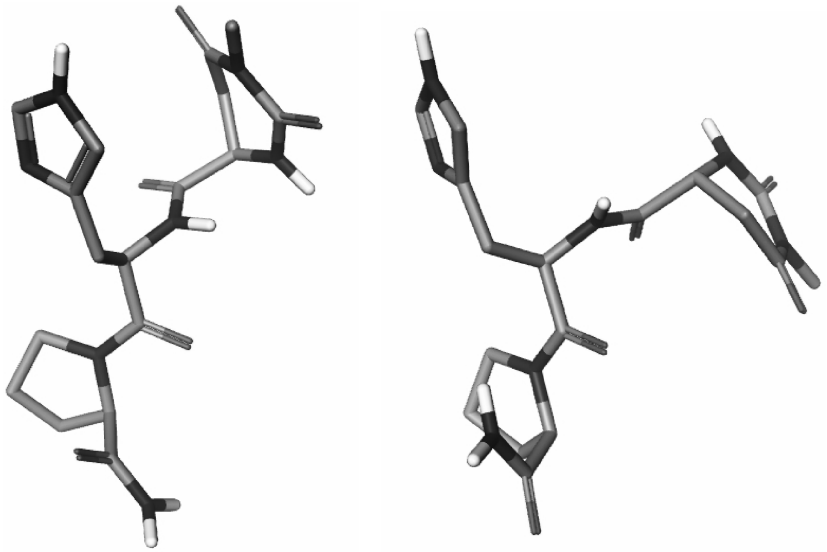

FIGURE 26.10 Conformations of taltireline α-form (a) and β-form (b). Only polar hydrogens are shown.

was not only influenced by the cooling rate but also affected by the solvent of crystallization. For example, form B was crystallized from a water solution with high initial drug concentration independent of the rate of cooling. Additionally, the stable form A was crystallized from methanol and acetonitrile solutions at low initial drug concentrations. No conformational population study in solutions was reported by the authors.

Conformational populations of forms A and B were predicted at a crystallization temperature of 50°C in three solvents at the PBE/DNP/COSMO level of theory. Due to the very high flexibility of the drug, crystallographic conformations (Figure 26.12) were adopted for the calculations with no conformational search. The resulting conformer population in three solvents is presented in Figure 26.13. It is demonstrated that in addition to any solubility and kinetic factors, the preference of crystallization of B or A conformers in different solvents can be accounted for by a trend in a conformational distribution. The conformer A displays the highest population in methanol and acetonitrile from which it was preferably crystallized. The population of the conformer B increases and becomes the highest in the water solution, from which it was crystallized.

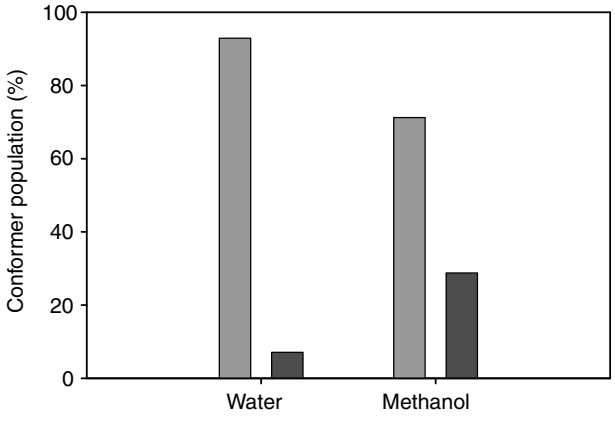

FIGURE 26.11 Predicted populations of the α-form (gray) and β-form (black) taltireline conformers in water and methanol.

26.3.2.4 Ritanovir Ritanovir, a HIV-protease inhibitor, is a well-known example of the impact polymorphism has on drug development [45]. Currently, two polymorphic forms, I and II, are known with form II being the most stable at room temperature. A solvent-mediated polymorphic conversion study was reported by Miller et al [39]. It was demonstrated that, although the slurry crystallization is preferentially thermodynamically controlled, relatively high drug solubility (>8 mM but <200 mM) is needed to ensure solvent-mediated conversion to the most stable form. These conclusions were supported by polymorph screening in 13 solvents. Conformational populations of forms I and II in 13 solvents were predicted at room temperature at the PBE/DNP/COSMO level of theory. Due to the extremely high flexibility of the ritanovir drug, the crystallographic conformations were adopted (Figure 26.14) for the calculations. The conformations were taken from CSD database (reference codes are YIGPIO and YIGPIO01). The resulting conformer populations together with the polymorph screening results are presented in Table 26.5. It is demonstrated that except for MTBE, the results of 2-week slurry crystallization follow the trend of the preferred conformer population in the corresponding solvent.

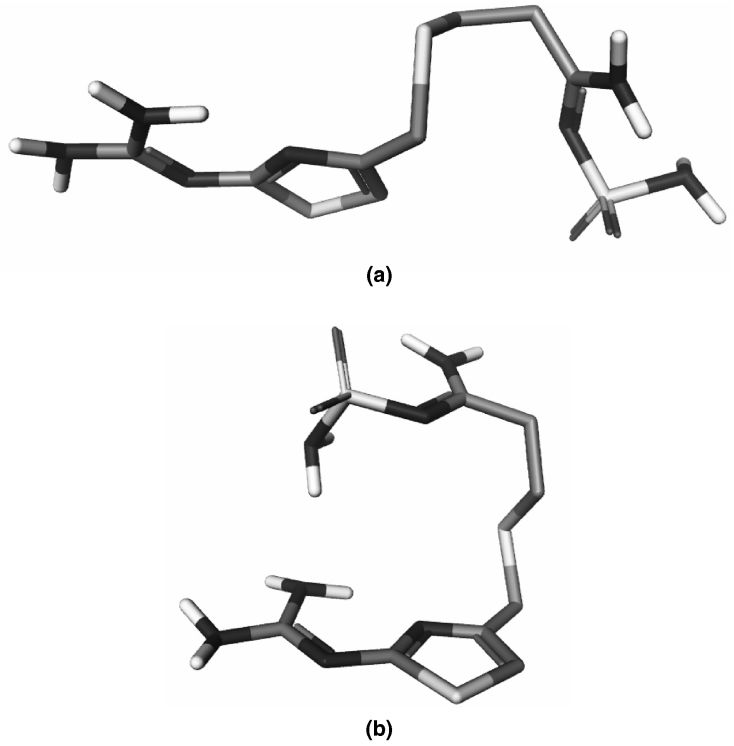

FIGURE 26.12 Molecular conformations of famotidine polymorphs A (a) and B (b). The crystal structures were taken from CSD, reference codes: FOGVIG04 (form A) and FOGVIG05 (form B). Only polar hydrogens are shown.

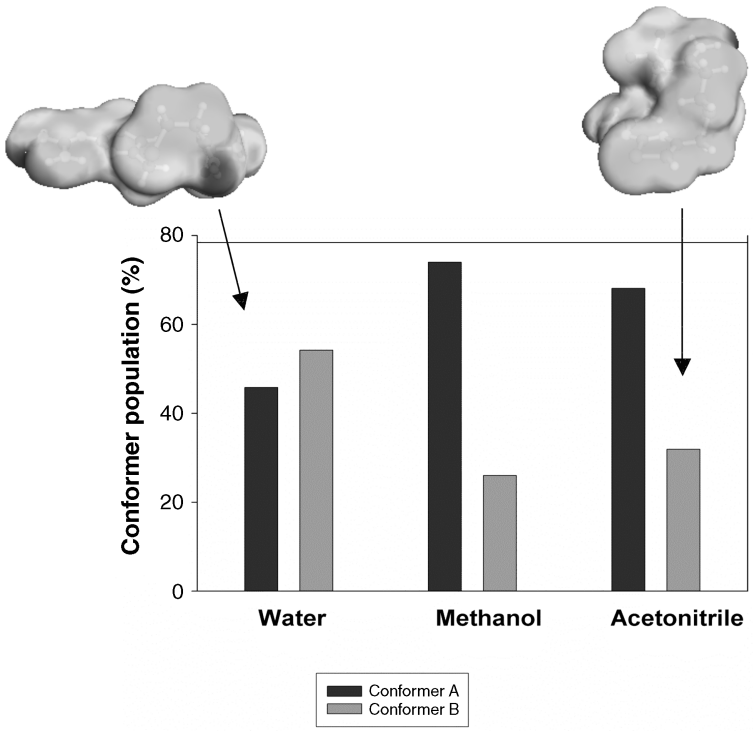

FIGURE 26.13 Histogram of predicted conformational distributions of famotidine in three solvents at 50°C. COSMO surfaces of the two conformers are shown on the top.

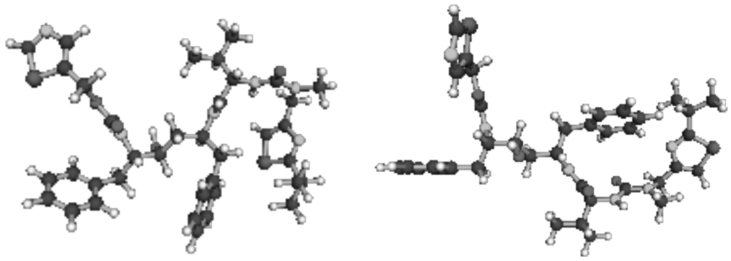

FIGURE 26.14 Crystallographic conformations of ritanovir forms I and II. The crystal structures were taken from CSD, reference codes: YIGPIO and YIGPIO01.

26.3.3 Implication to Crystal Structure Prediction

Crystal structure prediction is becoming a useful tool conducted in parallel to polymorph screening as well as being able to assess the risk of discovering a more stable form [15–18]. A starting point for CSP is the selection of molecular conformations that are as a rule held rigid during the generation of potential packing diagrams. Typically, the conformations are generated in the gas phase [19–21]. Since crystallization in the pharmaceutical industry is not performed from the gas phase but rather from different solvents, we recommend adopting the method of conformer distribution analysis, considered in this chapter, be applied to the conformations selection for virtual polymorph screening. For this, a diverse set of solvents should be considered in order to determine whether the solvent induces conformational switching of the active pharmaceutical. An indication that a molecule may switch conformations is the presence of intramolecular hydrogen bonding or a noticeable variation of molecular hydrophobic and hydrophilic surfaces. We propose a small diverse set of solvents to be considered for selecting molecular conformations used in CSP: polar protic—water (both HB donor and acceptor capabilities) and diethyl amine (HB donor capabilities); polar aprotic—acetone (HB acceptor capabilities); non-polar—hexane; and self-media to mimic solid amorphous. A combined set of conformations, which displayed the highest populations in any of the above solvents, can be recommended for the virtual conformational polymorph screening.

In order to illustrate this point, a conformer selection in support of CSP analysis was performed using a theoretical conformational population study of the flexible *S*-ibuprofen molecule. This study allowed for the selection of only four preferred conformations (Figure 26.8) with the highest populations using the following three solvents: methanol, acetone, and acetonitrile. Theoretical conformational distribution analysis in water, diethylamine, hexane, and self-media at the PBE/DNP/COSMO level of theory discover the same four favorable conformations. Thus, the selected four conformations can be used as a starting point for CSP. In addition, we should take into account that the acid group may rotate in the crystalline environment to participate in hydrogen-bonding interactions. This adds at least another four

TABLE 26.5 Results of Polymorph Screen of Ritanovir [39] and Predicted Conformer Populations at Room Temperature

Solvent	Solid Form (2 days)[a]	Solid Form (2 weeks)[a]	Conformer I Population[b] (%)	Conformer II Population[b] (%)
Water	I	II	21	79
Hexane	I	I,II mixture	85	15
Methyl-*t*-butyl ether	I	I	39	61
1,2-Xylene	I	I	70	30
Toluene	I	I	68	32
Nitromethane	II	II	31	69
Ethyl acetate	II	II	35	65
Acetonitrile	II	II	26	74
2-Propanol	II	II	32	68
2-Butanone	II	II	34	66
Acetone	II	II	27	73
1,2-Dimethoxyethane	II	II	28	72
Ethanol	II	II	30	70

[a] Results of stable polymorph screen reported by Miller et al. [39].
[b] Predictions at PBE/DNP/COSMO level of theory.

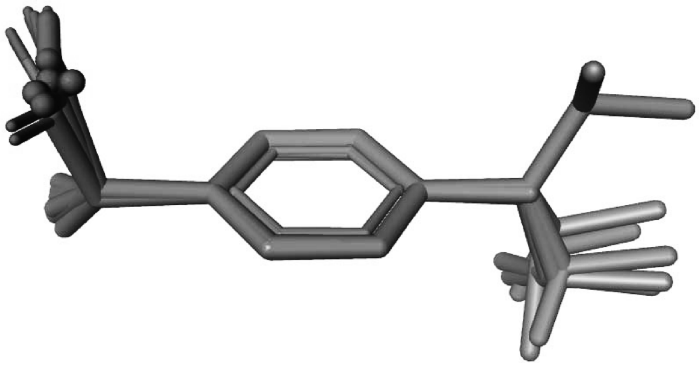

FIGURE 26.15 Alignment of the crystallographically observed *S*-ibuprofen conformations (CSD reference codes are IBPRAC, JEKNOC10, JEKNOC11, HUPPAJ, and RONWOG). All hydrogens are omitted.

conformations that are different from the initial set only by rotation of the acidic group by ~180°. In order to validate this selection process, the generated favorable conformers for *S*-ibuprofen (Figure 26.8) were compared with the observed molecular conformations from the Cambridge Structural Database (reference codes: IBPRAC, JEKNOC10, JEKNOC11, HUPPAJ, and RONWOG). Aligned crystallographic conformations are shown in Figure 26.15. An accuracy of the best alignment of the four selected favorable conformations (hydrogens are removed for the alignment) with those crystallographically observed is presented in Table 26.6. Quite low RMSD values demonstrate a good quality of theoretical selection of the conformations. It is interesting that while all crystallographic conformations were represented in the selected set of the favorable conformations of *S*-ibuprofen, one of the preferred conformations (conformer 3 in Table 26.3; Figure 26.8) has not yet been crystallographically observed (Figure 26.15).

26.4 CONCLUSIONS

Molecular crystallization is a very complex phenomenon, which is dependent on a combination of multiple thermodynamic and kinetic factors. Added complexity occurs when attempting to crystallize a conformational polymorph that is selected for drug development. In this study, we have shown the use of one parameter, such as relative conformer population, in exploring the possibility of controlling crystallization of conformational polymorphs. We have demonstrated that relative conformational population behavior in different solvents can be reasonably accurately predicted by theoretical methods. A correlation between trends of predicted (and, in some cases, also observed) conformational distribution changes in different solvents and crystallization results for conformational polymorphs were found in the four examples considered in this chapter. Although more extended testing is required, the following applications may be proposed.

1. The solvent selection strategy may focus on an attempt to diversify predicted conformer distribution in general, adopting crystallographic and/or theoretically generated conformations. This may facilitate crystallization of new form(s) that are both stable and metastable.
2. Another application of solvent selection is based on predicted change (increase or decrease) of the population(s) of the known conformer(s). This may allow tuning (promotion or inhibition) of the corresponding polymorph(s) crystallization.

In all cases, the final selection of solvents should also satisfy the criteria of relatively high (predicted or measured) solubility of the compound under consideration. In addition, the theoretical prediction of conformer distribution in different solvents, including self-media, was proposed for selection of preferable starting conformation(s) for virtual polymorph screening via crystal structure prediction.

TABLE 26.6 Best Alignments of the Calculated Favorable Conformations of *S*-Ibuprofen with the Similar Crystallographic Conformations from CSD

Conformer	RMSD (Å)	Reference Code
1	0.27	RONWOG
2	0.23	IBPRAC, JEKNOC10, JEKNOC11
4	0.12	HUPPAJ

ACKNOWLEDGMENTS

The authors would like to thank Mr. Brian Samas and Dr. Brian Marquez for the valuable comments and discussions.

Yuriy A. Abramov is thankful to Dr. Alex Goldberg for the valuable suggestions in running DMol^3 applications. YAA is grateful to Dr. Frank Eckert for the valuable consultations on COSMOtherm implementation of conformational population analysis.

REFERENCES

1. Bernstein J. *Polymorphism in Molecular Crystals*, Clarendon, Oxford, 2002.
2. Nangia A. Conformational polymorphism in organic crystals. *Acc. Chem. Res.* 2008;41:595–604.
3. Yu L, Reutzel-Edens SM, Mitchell CA. Crystallization and polymorphism of conformationally flexible molecules: problems, patterns, and strategies. *Org. Proc. Res. Dev.* 2000;4: 396–402.
4. Weissbuch I, Kuzmenko I, Vaida M, Zait S, Leiserowitz L, Lahav M. Twinned crystals of enantiomorphous morphology of racemic alanine induced by optically resolved α-amino acids: a stereochemical probe for the early stages of crystal nucleation. *Chem. Mater.* 1994;6:1258–1268.
5. Weissbuch I, Popoviz-Biro R, Leiswerowitz L, Lahav M. Lock-and-key processes at crystalline interfaces: relevance to the spontaneous generation of chirality. In: Behr J-P, editor. *The Lock-and-Key Principle: The State of the Art—100 Years On*, John Wiley & Sons, New York, 1994, pp. 173–246.
6. Lee AY, Lee IS, Dette SS, Boerner J, Myerson AS. Crystallization on confined engineered surfaces: a method to control crystal size and generate different polymorphs. *J. Am. Chem. Soc.* 2005;127:14982–14983.
7. Lee AY, Lee IS, Myerson AS. Factors affecting the polymorphic outcome of glycine crystals constrained on patterned substrates. *Chem. Eng. Tech.* 2006;29:281–285.
8. Weissbuch I, Addadi L, Leiswerowitz L. Molecular recognition at crystal interfaces. *Science* 1991;253:637–645.
9. Datta S, Grant DJW. Effect of supersaturation on the crystallization of phenylbutazone polymorphs. *Cryst. Res. Technol.* 2005;40:233–242.
10. Davey RJ, Blagden N, Righini S, Alison H, Ferrari ES. Nucleation control in solution mediated polymorphic phase transformations: the case of 2,6-dihydroxybenzoic acid. *J. Phys. Chem. B* 2002;106:1954–1959.
11. Davey RJ, Blagden N, Potts GD, Docherty R. Polymorphism in molecular crystals: Stabilization of a metastable form by conformational mimicry. *J. Am. Chem. Soc.* 1997;119: 1767–1772.
12. Mullin JW. *Crystallization*, Linacre House, Jordan Hill, Oxford, 1992.
13. Threlfall T. Structural and thermodynamic explanations of Ostwald's Rule. *Org. Proc. Res. Dev.* 2003;7:1017–1027.
14. Hursthouse MB, Huth S, Threlfall TL. Why do organic compounds crystallise well or badly or ever so slowly? Why is crystallization nevertheless such a good purification technique? *Org. Proc. Res. Dev.* 2009;13:1231–1240.
15. Blagden N, Davey RJ. Polymorph selection: challenges for the future? *Cryst. Growth Des.* 2003;3:873–885.
16. Cross WI, Blagden N, Davey, RJ, Pritchard, RG, Neumann, MA, Roberts, RJ, Rowe RC. A whole output strategy for polymorph screening: combining crystal structure prediction, graph set analysis, and targeted crystallization experiments in the case of diflunisal. *Cryst. Growth Des.* 2003;3:151–158.
17. Price SL. From crystal structure prediction to polymorph prediction: interpreting the crystal energy landscape. *Phys. Chem. Chem. Phys.* 2008;10:1996–2009.
18. Price SL. The computational prediction of pharmaceutical crystal structures and polymorphism. *Adv. Drug Del. Rev.* 2004;56:301–319.
19. Ouvrard C, Price SL. Toward crystal structure prediction for conformationally flexible molecules: the headaches illustrated by aspirin. *Cryst. Growth Des.* 2004;4:1119–1127.
20. Day GM, Motherwell WDS, Jones W. A strategy for predicting the crystal structures of flexible molecules: the polymorphism of phenobarbital. *Phys. Chem. Chem. Phys.* 2008;9: 1693–1704.
21. Cooper TG, Hejczyk KE, Jones W, Day GM. Molecular polarization effects on the relative energies of the real and putative crystal structures of valine. *J. Chem. The. Comput.* 2008;4:1795–1805.
22. Weng ZF, Motherwell WDS, Allen FH, Cole JM. Conformational variability of molecules in different crystal environments: a database study. *Acta Cryst*. 2008; *B64*:348–362.
23. MOE 2008.10, Chemical Computing Group, Inc., 1010 Sherbrooke Street West, Suite 910, Montréal, Québec, Canada. http://www.chemcomp.com
24. Delley B. An all-electron numerical method for solving the local density functional for polyatomic molecules. *J. Chem. Phys.* 1990;92:508–517.
25. Delley B. From molecules to solids with the DMol^3 approach. *J. Chem. Phys.* 2000;113:7756–7764.
26. Accelrys Software. Material Studio 4.4 DMol^3; Accelrys Software, Inc., San Diego, CA, 2008.
27. Perdew JP, Burke K, Ernzerhof M. Generalized gradient approximation made simple. *Phys. Rev. Lett.* 1996;77: 3865–3868.
28. Andzelm J, Kölmel C, Klamt A. Incorporation of solvent effects into density functional calculations of molecular energies and geometries. *J. Chem. Phys.* 1995;103:9312–9320.
29. Zhao Y, Truhlar DG. Benchmark databases of nonbonded interactions and their use to test density functional theory. *J. Chem. Theory Comput*. 2005;1:415–432.
30. Klampt A. *COSMO-RS: From Quantum Chemistry to Fluid-Phase Thermodynamics and Drug Design*, Elsevier, Amsterdam, 2005.
31. COSMOtherm, Version C2.1_0109, COSMOLogic GmbH, Leverkusen, Germany.
32. Lein M, Dobson JF, Gross EKU. Towards the description of van der Waals interactions within density functional theory. *J. Comput. Chem.* 1999;20:12–22.

33. Weigend F, Häser M, Patzelt H, Ahlrichs R. RI-MP2: optimized auxiliary basis sets and demonstration of efficiency. *Chem. Phys. Lett*. 1998;294:143–152.
34. TURBOMOLE, V6.0 2009, a development of University of Karlsruhe and Forschungszentrum Karlsruhe GmbH, 1989–2007, TURBOMOLE GmbH, since 2007.
35. Keeler J, Neuhaus D, Titman JJ. A convenient technique for the measurement and assignment of long-range carbon-13 proton coupling constants. *Chem. Phys. Lett*. 1988;146:545–548.
36. Yamasaki R, Tanatani A, Azumaya I, Masu H, Yamaguchi K, Kagechika H. Solvent-dependent conformational switching of *N*-phenylhydroxamic acid and its application in crystal engineering. *Cryst. Growth Des.* 2006;9:2007–2010.
37. Forbes CC, Beatty AM, Smith BD. Using pentafluorophenyl as a Lewis acid to stabilize a *cis* secondary amide conformation. *Org. Lett*. 2001;3:3595–3598.
38. Gu C, Young JrV, Grant DJW. Polymorphs screening: influence of solvents on the rate of solvent-mediated polymorphic transformation. *J. Pharm. Sci.* 2001;90:1878–1890.
39. Miller JM, Collman BM, Greene LR, Grant DJW, Blackburn AC. Identifying the stable polymorph early in the drug discovery–-development process. *Pharm. Dev. Technol.* 2005;10:291–297.
40. Ostwald W. Studien Uber Die Bildung und Umwandlung Fester Korper. *Z. Physik. Chem.* 1897;22:289–302.
41. Maruyama S, Ooshima H, Kato J. Crystal structures and solvent-mediated transformation of taltireline polymorphs. *Chem. Eng. J.* 1999;75:193–200.
42. Maruyama S, Ooshima H. Mechanism of the solvent-mediated transformation of taltirelin polymorphs promoted by methanol. *Chem. Eng. J.* 2001;81:1–7.
43. Allen FH, Bellard S, Brice MD, Cartwright BA, Doubleday A, Higgs H, Hummelink TWA, Hummelink-Peters BG, Kennard O, Motherwell WDS, Rodgers JR, Watson DG. The Cambridge Structural Database: a quarter of a million crystal structures and rising. *Acta Cryst*. 1979;B35:2331–2339.
44. Lu J, Wang X-J, Yand X, Ching C-B. Characterization and selective crystallization of famotidine polymorphs. *J. Pharm. Sci.* 2007;96:2457–2468.
45. Chemburkar SR, Bauer J, Deming K, Spiwek H, Patel K, Morris J, Henry R, Spanton S, Dziki W, Porter W, Quick J, Bauer P, Donaubauer J, Narayanan BA, Soldani M, Riley D, McFarland K. Dealing with the impact of ritonavir polymorphs on the late stages of bulk drug process development. *Org. Proc. Res. Dev.* 2000;4:413–417.